

Synthesis and Spectroelectrochemical Investigation of Low-Bandgap Polymer: Integrated Quinoxaline and Benzimidazole in One Electron Acceptor Unit

Mamtimin Mahmut, Tunsagul Awut, Ismayil Nurulla, Maxhur Mijit

Xinjiang University Key Laboratory of Functional Polymer Materials, College of Chemistry and Chemical Engineering, Xinjiang University, Urumqi 830046, China

Correspondence to: I. Nurulla (E-mail: ismayilnu@sohu.com)

ABSTRACT: Two novel π -conjugated monomers, 6-(4-octyloxyphenyl)-4,8-bis(thiophene-2-yl)-3H-[d] imidazole[1,2,5] benzothiadiazole (M3) and 4-(4-octyloxyphenyl)-2,6-bis(thiophene-2-yl)-3H-[d] imidazole-acenaphtho[1,2-b]quinoxaline (M4), were synthesized. The monomer M4 contains a thiophene electron-donating unit and electron withdrawing unit in which quinoxaline and benzimidazole integrated in one benzene ring. Electrochemical polymerization of the monomers was carried out in acetonitrile/dichloromethane solvent mixture containing tetra-*n*-butylammonium hexafluorophosphate and electrochromic properties of polymers (P3 and P4) are described in this article. Furthermore, the effects of structural difference on electrochemical redox behavior and spectroelectrochemical properties of the two resulting polymers were examined. The results showed that an anodic wave at +0.48 V versus Ag wire pseudo-reference electrode corresponding to the monomer M4 oxidation was observed, while one anodic wave at +0.70 V was observed in oxidation of M3 as it contains stronger electron withdrawing thiadiazole structure. The UV-vis-Near-infrared (Near-infrared spectroscopy) (NIR) spectra analysis revealed that the two polymers have one absorbance band centered at 603 nm. The band gaps, defined as the onset of the absorption band at 603 nm of these polymers, were determined as 1.60 eV for P3 and as 1.55 eV for P4. The electrochromic results showed that P3 revealed about 20% optical contrast at 980 nm and the P4 has 30% optical contrast at 806 nm with low response time (1 s for each polymer). © 2014 Wiley Periodicals, Inc. *J. Appl. Polym. Sci.* **2014**, *131*, 40861.

KEYWORDS: characterization; conducting polymers; electrochemistry; spectroelectrochemical properties

Received 24 November 2013; accepted 12 April 2014

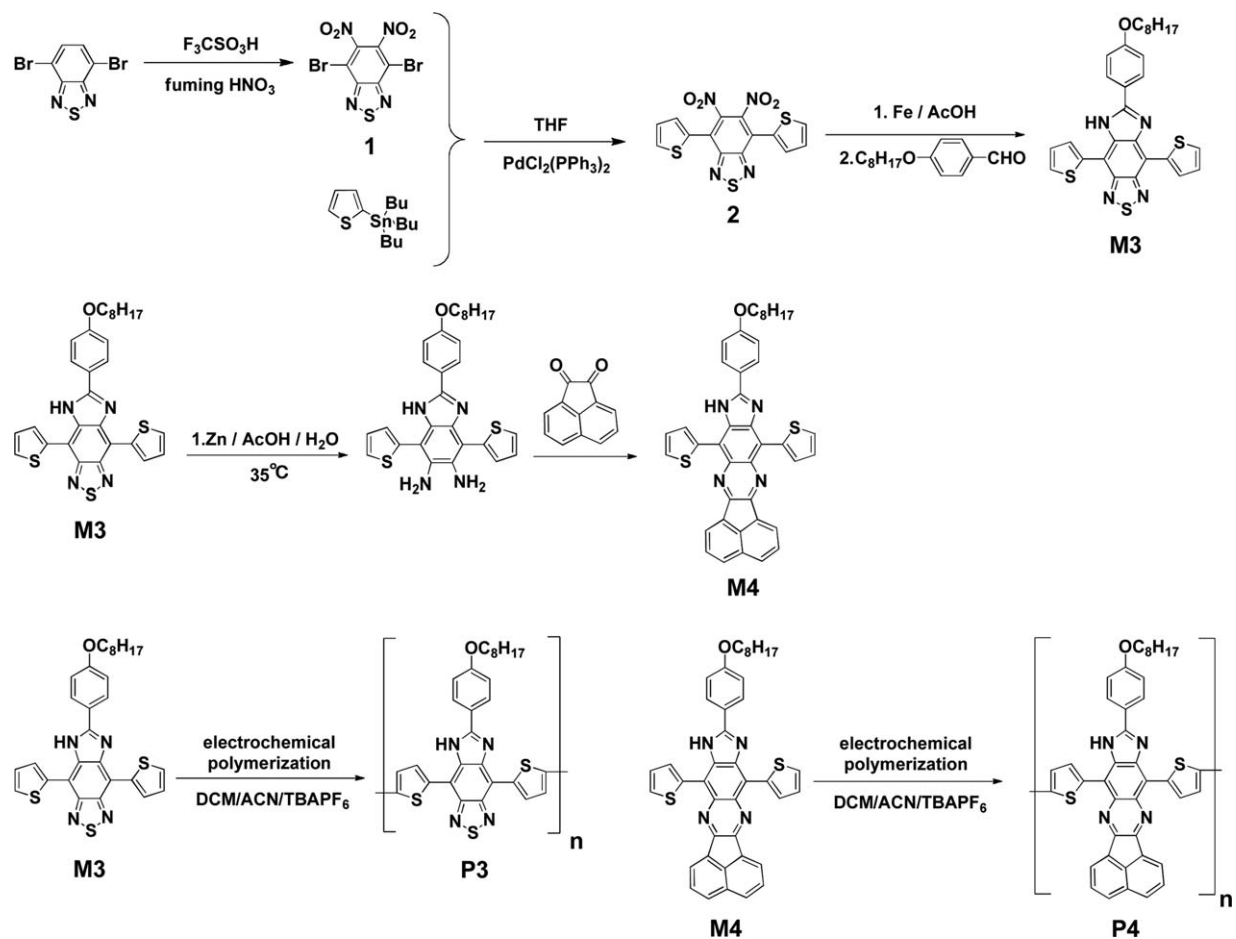
DOI: 10.1002/app.40861

INTRODUCTION

Electrochromism involves electroactive materials that show a reversible color change when a small DC voltage is applied. The electrochromic materials include inorganic and organic materials. The inorganic materials are mainly metal oxides such as WO_3 , NiO_2 , and TiO_2 , and the organic materials include small molecules and conjugated polymers.^{1–3} Among conjugated polymers, low-band gap polymers obtained by electrochemical polymerization of suitable redox active monomers draw considerable attention at present due to their potential ability in visible, IR, and microwave electrochromics. This type of polymers can be used in photoelectric devices such as electrochromic displays, vision systems, or smart windows.^{4,5} In recent years, many studies on the design and synthesis of low-band gap electrochromic polymers have been carried out due to their unique optoelectronic properties. In these studies, the most used method to obtain low-bandgap is the donor–acceptor approach.^{6–11} Some works

reported that low-bandgap polymers containing quinoxaline as an acceptor unit demonstrated good electrochromic ability.^{12–20} These polymers generally show a variety of excellent properties such as distinct optical changes throughout the visible region, short switching time, and low-voltage electrochromic response (i.e., potential lower than 1.3 V).

Among a wide variety of acceptor units, benzimidazole unit has also been shown to be an excellent building block for synthesis of low-bandgap conjugated polymers. Benzimidazole-containing polymers and copolymers were synthesized and characterized by several research groups.²¹ Electrochromic investigation of electrochemically polymerized benzimidazole-containing donor–acceptor type polymers was first reported by Akpınar et al.²² Ozdemir et al. reported the synthesis of several monomers by combining benzotriazole and quinoxaline units in an acceptor unit and polymerized electrochemically to obtain multipurpose donor–acceptor type polymers. These polymers revealed both



Scheme 1. Schematic route for the synthesis of monomer.

p- and *n*-type doping properties and excellent electrochromic properties.²³ Nurioglu et al. also reported the synthesis of several new material which containing benzimidazole as acceptor and these materials exhibits good electrochromic properties.²⁴ From the results of these previous researches, we conclude that low-bandgap materials which contain quinoxaline or benzimidazole units as acceptors are excellent materials for electrochromic devices. However, quinoxaline or benzimidazole structure is used separately in these studies as the electron acceptor unit. How will the electrochromic properties of the polymers be if the quinoxaline and benzimidazole are integrated in one electron acceptor unit? So, in this study, we designed and synthesized two new monomers 6-(4-octyloxyphenyl)-4,8-bis(thiophene-2-yl)-3H-[d]imidazole[1,2,5]benzothiadiazole (M3) and 4-(4-octyloxyphenyl)-2,6-bis(thiophene-2-yl)-3H-[d]imidazole-acenaphtho [1,2-b]quinoxaline (M4). The monomer M4 was synthesized using M3 as raw material and it contains a thiophene electron-donating unit and electron withdrawing unit in which quinoxaline and benzimidazole integrated in one benzene ring. The two monomers were polymerized by electrochemical polymerization method on indium tin oxide (ITO)-coated glass slide to investigate the spectroelectrochemistry as well as switching properties of the polymers (Scheme 1).

EXPERIMENTAL

Materials and Equipments

All chemicals were purchased from Shanghai Boka Chemical Co. and used as received unless otherwise noted. Dry tetrahydrofuran (THF) was distilled over sodium with addition of benzophenone. 4,7-dibromo-5,6-dinitrobenzo[1,2,5]thiadiazole, 4,7-di(thiophene-2-yl)-5,6-dinitrobenzo[1,2,5]thiadiazole and *p*-octyloxybenzaldehyde were synthesized according to the literature procedures.^{25–27} The tetra-*n*-butylammonium hexafluorophosphate (TBAPF₆) electrolyte dissolved in the solvent mixture of dichloromethane (DCM) and acetonitrile (ACN) and was used as supporting electrolyte solution in electrochemical polymerization and spectroelectrochemistry analysis process.

A Zahner-Zennium (Germany) electrochemical workstation was used for all electrochemical studies. Electrochemical polymerization was performed in a three-electrode cell consisting of an ITO glass as the working electrode, platinum wire as the counter electrode, and Ag wire as pseudo-reference electrode. Electronic absorption spectra and electrochromic switching of polymers were taken with a Shimadzu UV-3600 UV-Vis-Near-infrared (Near-infrared spectroscopy) (NIR) Spectrophotometer linked with a MCP-1 Potentiostat (Jiangsu Jianguan, China). ¹H-NMR

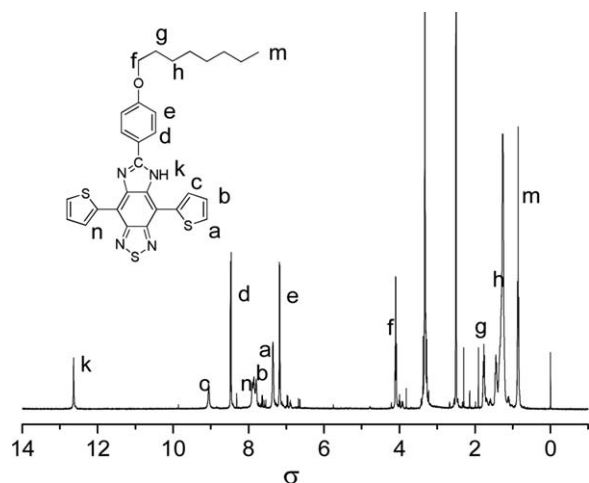


Figure 1. $^1\text{H-NMR}$ spectra of monomer M3.

spectra of monomers were recorded in CDCl_3 on VARIAN INOVA-400 spectrometer (400 MHz). Chemical shifts were given in ppm downfield from tetramethylsilane.

6-(4-octyloxyphenyl)-4,8-bis(thiophene-2-yl)-3H-[d]imidazole[1,2,5]benzothiadiazole (M3)

A mixture of 4,7-dibromo-5,6-dinitro-benzo (383 mg, 1 mmol) and iron powder (750 mg) in acetic acid was stirred for 3.5 h at 80°C . Then, the reaction mixture was poured into water (250 mL) to precipitate and extracted by diethyl ether. The diethyl ether solution was washed with brine and dried with Mg_2SO_4 . After the solvent was removed, the residue was dissolved in acetic acid (25 mL), *p*-octyloxybenzaldehyde (416 mg, 2 mmol) was added to the solution and refluxed for 72 h. After that the reaction mixture poured into water and extracted by CHCl_3 . The organic phase was washed with NaHCO_3 solution, water, and dried with Mg_2SO_4 . After removing the organic solvents, the crude product was purified on a silica gel column [CHCl_3 : petroleum ether($60\text{--}90^\circ\text{C}$) = 1 : 2 as eluent] to give the desired product M3 as red powder (356 mg, 65%). $^1\text{H NMR}$

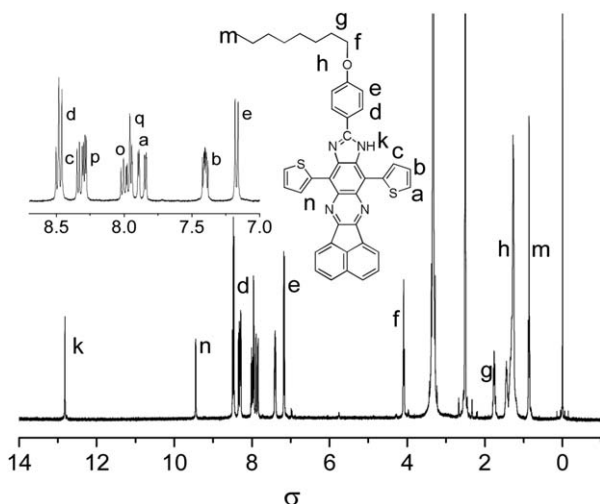


Figure 2. $^1\text{H-NMR}$ spectra of monomer M4. [Color figure can be viewed in the online issue, which is available at wileyonlinelibrary.com.]

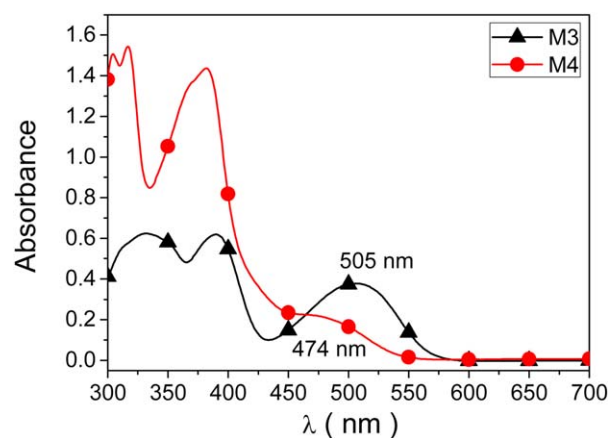


Figure 3. UV-vis-NIR spectra of M3 and M4 in DCM. The concentration of the monomers is $c = 3.0 \times 10^{-5}$ mol/L for M3 and $c = 1.2 \times 10^{-4}$ mol/L for M4. [Color figure can be viewed in the online issue, which is available at wileyonlinelibrary.com.]

(400 MHz, dimethyl sulfoxide (DMSO)) δ : 12.62 (s, 1H); 8.46 (d, $J = 8.8$ Hz, 2H); 7.90–7.85 (t, 2H); 7.80 (d, $J = 3.8$ Hz, 2H); 7.35 (d, $J = 4.5$ Hz, 2H); 7.17 (d, $J = 8.8$ Hz, 2H); 4.11–4.08 (m, 2H); 1.78–1.74 (m, 2H); 1.44–1.25 (m, 10H); 0.89–0.84 (m, 3H). UV-vis (CHCl_3): $\lambda_{\text{max}} = 328, 389, 506$ nm.

4-(4-octyloxyphenyl)-2,6-bis(thiophene-2-yl)-3H-[d]imidazole-acenaphtho[1,2-b]quinoxaline (M4)

To a mixture of 3 (544 mg, 1.0 mmol) and zinc dust (1.31 g, 20.0 mmol) in acetic acid (50 mL), a few drops of water was added and stirred at 35°C for 6 h, the color changed from red to pink. The solution was filtered twice and acenaphthylenequinone (200 mg, 1.1 mmol) was added to the pink solution, then the solution was stirred for 48 h at room temperature, after which it was poured into water and was extracted by CHCl_3 and the organic phase was dried over MgSO_4 . After removing the organic solvents, the crude product was purified on a silica gel column [CHCl_3 : petroleum ether ($60\text{--}90^\circ\text{C}$) = 2 : 1 as eluent] to give the desired product M4 as dark red powder (440 mg, 68%). $^1\text{H NMR}$ (400MHz, DMSO) δ : 12.82 (s, 1H); 8.46 (d, $J = 9.2$ Hz, 2H); 8.30–8.27 (m, 2H); 8.02–7.98 (m, 2H); 7.95–7.88 (m, 2H); 7.85–7.83 (m, 2H); 7.42–7.38 (m, 2H); 7.18 (d, $J = 8.8$ Hz, 2H); 4.10–4.07 (m, 2H); 1.77–1.74 (m, 2H); 1.44–1.26 (m, 10H); 0.87–0.84 (m, 3H). UV-vis (CHCl_3): $\lambda_{\text{max}} = 314, 383, 481$ nm.

RESULTS AND DISCUSSION

Synthesis and Characterization

The synthetic route toward the monomer and polymer are shown in Scheme 1.

The reagent 4,7-dibromo-5,6-dinitro-benzo[1,2,5]thiadiazole (1) was synthesized by the nitration of 4,7-dibromo-benzo[1,2,5]-thiadiazole using a mixture of fuming HNO_3 and $\text{CF}_3\text{SO}_3\text{H}$ as the previously described method. 4,7-Di(thiophene-2-yl)-5,6-dinitro-benzo[1,2,5]thiadiazole (2) was synthesized through Stille coupling reaction of 1 and 2-(tributylstanny)thiophene in freshly distilled THF with $\text{Pd}(\text{PPh}_3)_2\text{Cl}_2$ as the catalyst under nitrogen atmosphere in good yield. M3 was reduced with zinc

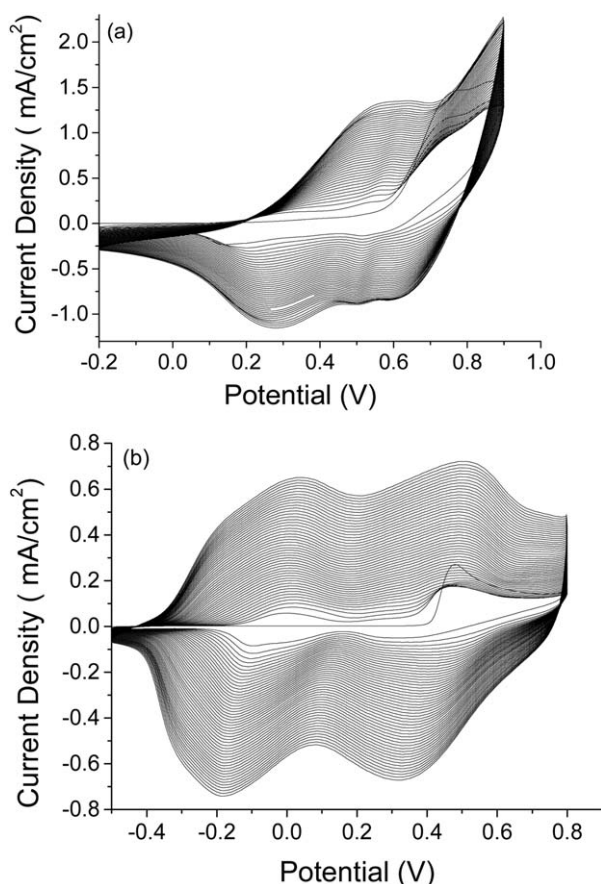


Figure 4. Cyclic voltammogram of (a) M3 in 0.1 M TBAPF₆/ACN/DCM (53/47, v/v) and (b) M4 in 0.1 M TBAPF₆/ACN/DCM (5/95, v/v) solution containing 50 mM monomer at scan rate of 100 mV/s. [Color figure can be viewed in the online issue, which is available at wileyonlinelibrary.com.]

powder to give the amine, and its condensation reaction with acenaphthylenequinone in acetic acid was performed to give M4.

¹H-NMR spectrum of M3 is shown in Figure 1. All of the detected peaks are consistent with the proposed structure. The signals at *f* (4.11–4.08 ppm), *g* (1.78–1.74 ppm), *h* (1.44–1.25 ppm), and *m* (0.89–0.84 ppm) arise due to the existence of three types of methylene and one type of methyl protons. Peaks *d* (8.48–8.45 ppm) and *e* (7.18–7.16 ppm) correspond to four protons on benzene ring. Peaks *a* (7.90 ppm), *b* (7.85–7.80 ppm), and *c* (9.05 ppm) implies the presence of protons on thiophene rings. Peak at *k* (12.62 ppm) is assigned to the proton of amine in imidazole ring.

¹H-NMR spectrum of M4 is shown in Figure 2. The signals at *f* (4.10–4.07 ppm), *g* (1.77 ppm), *h* (1.44–1.27 ppm), and *m* (0.87–0.84 ppm) arise due to the existence of three types of methylene and one type methyl protons. Peaks *d* (8.48–8.45 ppm) and *e* (7.18–7.15 ppm) correspond to four protons on benzene ring. Peaks *a* (7.88–7.83 ppm), *b* (7.42–7.38 ppm), *c* (8.34–8.33 ppm), and *n* (9.45–9.44 ppm) implies the presence of protons on thiophene rings. Peaks *o* (8.02–7.97 ppm), *p* (8.30–8.27 ppm), and *q* (7.95–7.94 ppm) are assigned to the protons of acenaphtho ring. Peak at *k* (12.8 ppm) is assigned to the proton of amine in

imidazole ring. ¹H-NMR results reveal that the presumed structure was obtained.

Optical Properties of Monomers

The solution state UV–vis absorption spectra for the two monomers can be seen in Figure 3. The concentration of the monomers is 3.0×10^{-5} mol/L for M3 and 1.2×10^{-4} mol/L for M4. All of the monomers showed three distinct absorption bands: the band around 300–500 nm can be assigned to the π - π^* transition. M4 exhibited a side peak at 474 nm and the maximum absorption of M3 is located at 505 nm, which is red shifted 29 nm in compared with the peak of M4. The red shift in this intramolecular charge transfer band can be attributed to the nature of electron acceptor units in two aspects. The acenaphtho structure in M4 has larger planer conjugation than the thiadiazole structure in M3 and the absorption peaks of M4 should appear at longer wavelength than M3. However, the experiment exhibits an opposite result. This is because the steric repulsion between the thiadiazole structure and thiophene unit is lower than that between the acenaphtho structure and thiophene unit, which leads to a planar geometry. The second aspect might be the presence of two lone pair on the sulfur atom in thiadiazole increases the electron cloud density of electron acceptor unit of M3, and it leads to greater π -conjugation of M3. These arguments conclude that M3 has a coplanar backbone, and enhanced π -delocalization, which lead to a red-shifted absorption maximum in the visible region.

Electrochemistry

We investigated the redox behaviors of M3 and M4 using cyclic voltammetry at room temperature in a conventional three electrode cell, using ITO glass as the working electrode, platinum wire as the counter electrode, and Ag wire as pseudo-reference electrode (Figure 4). Electrochemical studies of M3 and M4 were performed in ACN/DCM solvent mixture using 0.1 M TBAPF₆ as supporting electrolyte. The ratios of solvent mixture are 53/47 (v/v) for M3 and 5/95 (v/v) for M4. The concentration of all monomers used for electrochemical polymerization was 0.01 M.

Electrochemical polymerization of M3 on ITO electrode was performed by applying potentials between -0.2 and $+0.9$ V at a scan rate of 100 mV/s. During the first anodic scan the onset of oxidation starts at $+0.6$ V and one anodic wave was observed at $+0.70$ V [Figure 4(a)]. Subsequent cycling leads to one redox couple at $+0.38$ and $+0.19$ V associated with the oxidation and reduction of the polymers deposited on the ITO electrode surface. In Figure 4(a), the increase in current density with the number of scans clearly shows the deposition of an electroactive film of P3 on ITO followed by the oxidation peak increased to $+0.65$ V and the reduction peak increased to $+0.28$ V, respectively.

The potential using in multiple scan voltammetry for the electrochemical polymerization of M4 was from -0.5 to $+0.8$ V at a scan rate of 100 mV/s. During the first anodic scan the onset of oxidation starts at $+0.41$ V, and a single peak was observed at $+0.48$ V which corresponds to irreversible oxidation of the monomer [Figure 4(b)]. The subsequent cycle leads to two new redox couple associated with the oxidation and reduction of the

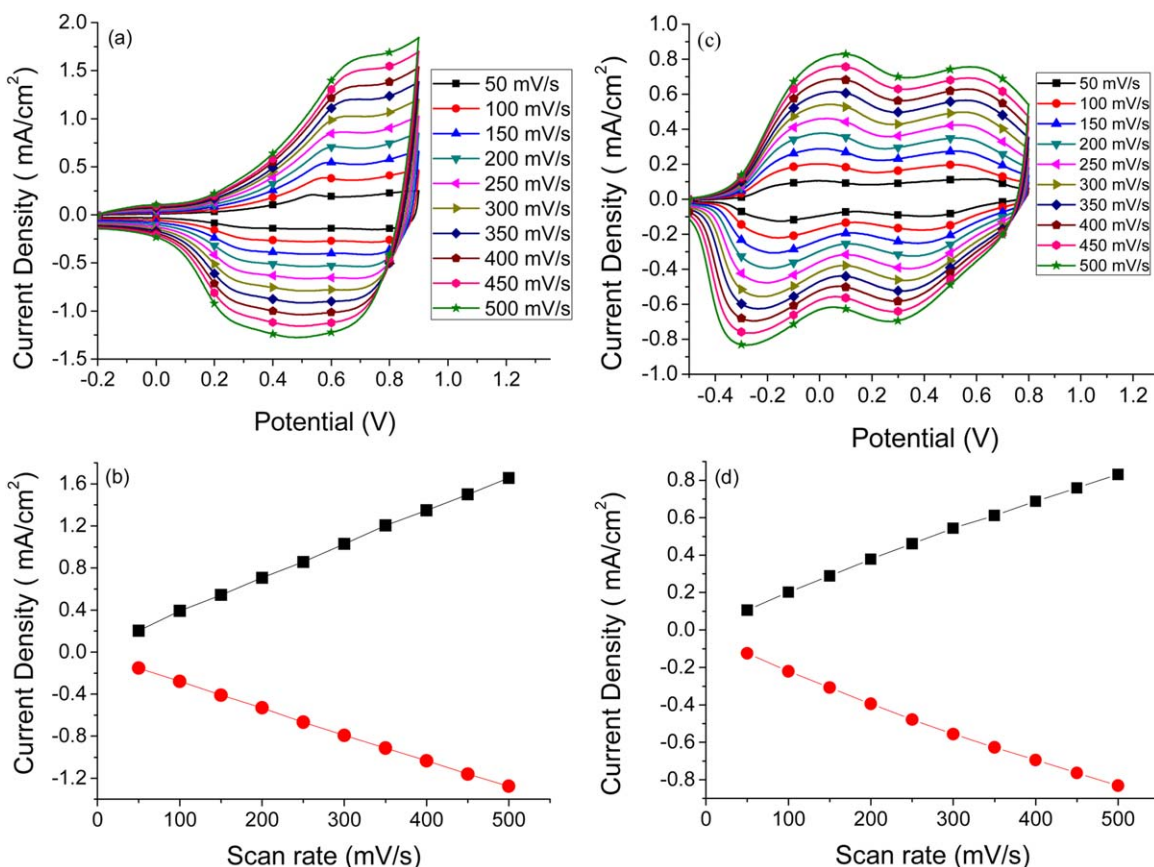


Figure 5. Scan rate dependence of (a) P3 and (c) P4 in monomer free ACN/DCM (5/95) solution containing 0.1M TBAPF₆ at scan rates of 50, 100, 150, 200, 250, 300, 350, 400, 450, and 500 mV/s. Relationship of anodic (■) and cathodic (●) current peaks as a function of scan rate for (b) P3 and (d) P4 film. [Color figure can be viewed in the online issue, which is available at wileyonlinelibrary.com.]

polymers deposited on the ITO electrode surface. The oxidation peak appears at 0 and +0.46 V, and the reduction peak appears at -0.08 and +0.34 V, respectively. On repeated scanning increasing current response of the polymer, redox process illustrates that electrochemical polymerization is proceeding at the electrode surface to form an electroactive polymer film.

The cyclic voltammogram results showed that the oxidation potential of M4 and P4 are lower than that of M3 and P3 measured under the described conditions, this lower potential can be attributed to difference of acceptor unit. The electron-withdrawing strength of thiadiazole structure in acceptor unit of M3 is stronger than the quinoxaline structure of M4.^{17,28} Thus, the electron acceptor unit of M3 became more electron-deficient and it increases the charge mobility from thiophene to electron acceptor unit. So, the electron density of thiophene ring in M3 was decreased and it leads to an increase in the oxidation potential of M3.

The scan rate dependences of the anodic and cathodic peak currents of polymers were studied in a monomer-free electrolyte solution. A linear relationship between the peak current and scan rate demonstrates that the films were well adhered and maintain reversible redox properties even at high scan rates acquiring rapid charge/discharge process (Figure 5).

Electrochromic Studies of Polymers

After electrochemical polymerization of M3 and M4 onto ITO surface, we treated the polymer P3 and P4 with phenylhydrazin for 3 h and examined the spectroelectrochemical properties.

Figure 6(a) shows the spectroelectrochemical series for p-doping of P3 between -0.2 and +0.8 V. The neutral form of the P3 is light blue in color, having one absorbance peak centered at 603 nm in electronic absorption spectra. Stepwise oxidation of the polymer film shows that the intensity of $\pi-\pi^*$ transition decreased as the color changes from blue to light reddish purple. On oxidation, absorption bands intensity at 603 nm decreased and absorption peaks red shifted when the potential changes from -0.2 to +0.8 V, finally appear at 532 nm. Meanwhile, there appear one new absorption peak in the region from 700 to 1100 nm and the maximum absorption peak centered at 980 nm.

The spectroelectrochemical series for p-doping of P4 were recorded at varies applied potential between -0.4 and +0.7 V [Figure 6(b)]. Oxidation of an electrochromic material produces radical cations and further oxidation produces dication, allowing new electronic transitions thereby changing the absorption spectra. The absorbance assigned to $\pi-\pi^*$ transitions for neutral form of P4 is at 603 nm. Stepwise oxidation of the P4 film

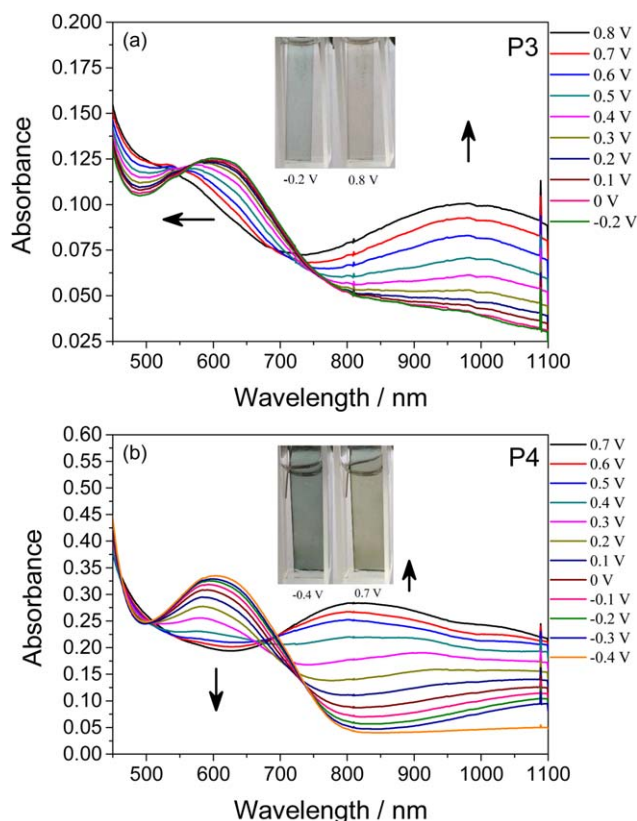


Figure 6. Electronic absorption spectra of (a) P3 and (b) P4 on ITO in 0.1 M TBAPF₆/ACN/DCM (5/95,v/v) at various applied potentials between -0.2 and 0.8 V for P3 and between -0.4 and 0.7 V for P4. [Color figure can be viewed in the online issue, which is available at wileyonlinelibrary.com.]

shows that absorption bands intensity at 603 nm decreased as the color changes from blue to yellow brown. These decrease as the doping proceeds while new absorbance bands evolve in the region from 630 to 1100 nm. The maximum absorption peak appeared at 1092 nm when the applied potential was -0.3 V. The absorption bands intensity increased and the absorption peaks blue shifted while the potential changes from -0.1 to $+0.7$ V and eventually appear at 806 nm, blue shifted about 286 nm. Conversely, a similar derivative which contains only acenaphthylquinoxaline structure as electron acceptor unit has a broad absorption band evolve at 1700 nm.¹³ Another similar derivative in which the electron acceptor unit is benzo[d]imidazole structure also has a broad absorption band appeared at 1120 nm.²⁴ As compared to the two type electron acceptor unit, the electron withdrawing unit of P3 and P4 has an absorption band at the shorter wavelength. This result indicates that when imidazole structure were combined with thiadiazole and quinoxaline structure, respectively, in a benzene ring at the same time, there exists four N atoms and the electron withdrawing unit has stronger electron-deficient than the reported structure. During the stepwise oxidation the acceptor unit became more electron-deficient and it may increase the molecular orbital energy, so the absorption peak blue shifted. The band gap (E_g), defined as the onset of the absorption band at 603 nm of the two polymers film, were calculated as 1.6 eV for P3 and 1.55 eV for P4.

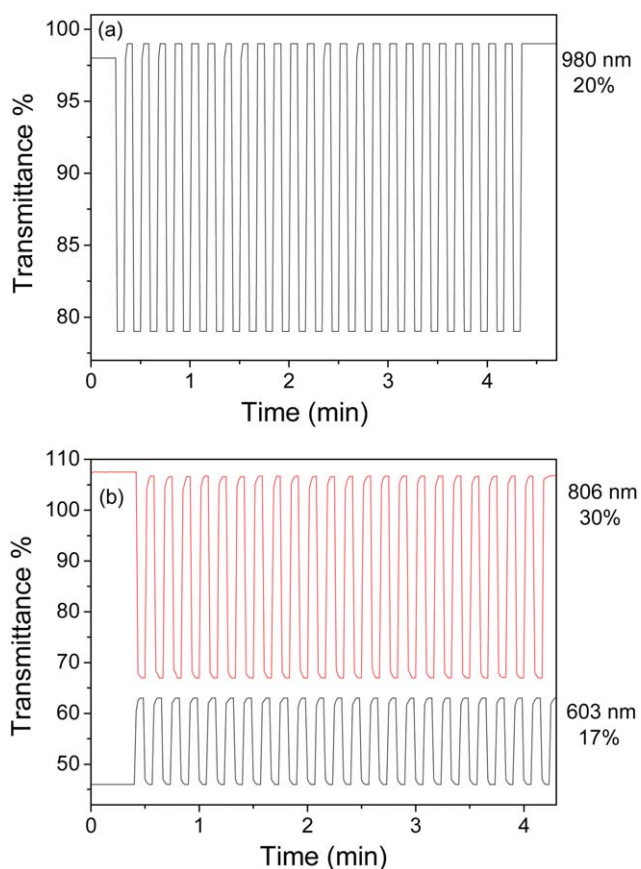


Figure 7. Optical transmittance changes for (a) P3 at 980 nm and (b) P4 at 603 and 806 nm in TBAPF₆/ACN/DCM (5/95,v/v) while the polymers switched between -0.2 and 0.8 V for P3 and between -0.4 and 0.7 V for P4 with a switch time of 5 s. [Color figure can be viewed in the online issue, which is available at wileyonlinelibrary.com.]

Electrochromic Switching

Electrochromic switching studies of P3 and P4 were performed while the potential was stepwise switched between -0.2 and $+0.8$ V for P3 and between -0.4 and $+0.7$ V for P4, the neutral and oxidized states with a residence time of 5 s (as shown in Figure 7). The optical switching studies were investigated using a square wave potential step method coupled with optical spectroscopy in a monomer free solution. During the experiment, the % transmittance at the wavelength of maximum contrast was measured by a UV-vis spectrophotometer. The optical contrast measured as the difference between % T in the neutral and oxidized forms (% ΔT) were found to be 20% at 980 nm for P3. Furthermore, the switching times was calculated as 1 s for this polymer. At the same condition, the optical contrast was determined for P4 as 17% at 603 nm and 30% at 806 nm with 1 s switching times.

CONCLUSIONS

In conclusion, two novel low band gap electroactive donor-acceptor type π -conjugated monomers consisting of thiophene as the donor unit and imidazole[1,2,5] benzothiadiazole and imidazole-acenaphtho [1,2-b]quinoxaline as the acceptor units were synthesized via a Stille coupling reaction and its electrochemical polymerizations were achieved on ITO-coated glass

slides to determine the optoelectronic properties of the polymers. The spectroelectrochemical and electrochromic switching properties of these polymers were studied. The experimental results showed that both polymers have electrochromic ability in visible and NIR region. P3 revealed about 20% optical contrast at 980 nm, whereas P4 exhibits 17% optical contrast at 603 nm and 30% at 806 nm with 1s switch times. Optical properties were compared with those of previously reported donor–acceptor–donor type π -conjugated polymers. The π – π^* absorption band of the polymers were observed at a shorter wavelength than those Donor–Acceptor–Donor type polymers which contains only imidazole or quinoxaline as acceptor unit.

ACKNOWLEDGMENTS

The authors gratefully acknowledge support from the National Natural Science Foundation of China (Nos. 20974092, 21164011) and Xinjiang University-Institute joint project (No. XY110112). The authors are also greatly indebted to Mr. Wan Fu Sun for his contribution to the analysis of spectra.

REFERENCES

1. Su, L.; Fang, J.; Lu, Z. *J. Appl. Polym. Sci.* **1998**, *70*, 1955.
2. Inamdar, A. I.; Sonavane, A. C.; Pawar, S. M.; Kim, Y.; Kim, J. H.; Patil, P. S.; Jung, W.; Im, H.; Kim, D.-Y.; Kim, H. *Appl. Surf. Sci.* **2011**, *257*, 9606.
3. Huang, J.-H.; Tzuyu Huang, A.; Hsu, C.-Y.; Lin, J.-T.; Chu, C.-W. *Sol. Energy Mater. Sol. Cells* **2012**, *98*, 300.
4. Sahin, E.; Sahmetlioglu, E.; Akhmedov, I. M.; Tanyeli, C.; Toppare, L. *Org. Electron.* **2006**, *7*, 351.
5. Chandrasekhara, P.; Zaya, B. J.; McQueeney, T.; Birur, G. C.; Sitaramc, V.; Menonc, R.; Coviello, M.; Elsenbaumerd, R. L. *Synth. Met.* **2005**, *155*, 623.
6. Lee, Y.; Nam, Y. M.; Jo, W. H. *J. Mater. Chem.* **2011**, *21*, 8583.
7. Ünür, E.; Toppare, L.; Yağcı, Y.; Yilmaz, F. *J. Appl. Polym. Sci.* **2005**, *95*, 1014.
8. Ak, M.; Camurlu, P.; Yilmaz, F.; Cianga, L.; Yağcı, Y.; Toppare, L. *J. Appl. Polym. Sci.* **2006**, *102*, 4500.
9. Bingöl, B.; Camurlu, P.; Toppare, L. *J. Appl. Polym. Sci.* **2006**, *100*, 1988.
10. Yi-Jie, T.; Hai-Feng, C.; Wen-Wei, Z.; Zhao-Yang, Z. *J. Appl. Polym. Sci.* **2013**, *127*, 636.
11. Zhao-yang, Z.; Yi-jie, T.; Xiao-qian, X.; Yong-jiang, Z.; Hai-feng, C.; Wen-wei, Z. *J. Appl. Polym. Sci.* **2013**, *129*, 1506.
12. Matsidik, R.; Mamtimin, X.; Mi, H. Y.; Nurulla, I. *J. Appl. Polym. Sci.* **2010**, *118*, 74.
13. Uduma, Y. A.; Durmus, A.; Gunbas, G. E.; Toppare, L. *Org. Electron.* **2008**, *9*, 501.
14. Pamuk, M.; Tirkeş, S.; Cihaner, A.; Algi, F. *Polymer* **2010**, *51*, 62.
15. Tarkuc, S.; Unver, E. K.; Udum, Y. A.; Toppare, L. *Eur. Polym. J.* **2010**, *46*, 2199.
16. Esmer, E. N.; Tarkuc, S.; Udum, Y. A.; Toppare, L. *Mater. Chem. Phys.* **2011**, *131*, 519.
17. Unver, E. K.; Tarkuc, S.; Baran, D.; Tanyeli, C.; Toppare, L. *Tetrahedron Lett.* **2011**, *52*, 2725.
18. Kivrak, A.; Carbas, B. B.; Zora, M.; Önal, A. M. *React. Funct. Polym.* **2012**, *72*, 613.
19. Sendur, M.; Balan, A.; Baran, D.; Karabay, B.; Toppare, L. *Org. Electron.* **2010**, *11*, 1877.
20. Sendur, M.; Balan, A.; Baran, D.; Toppare, L. *J. Polym. Sci. Part A: Polym. Chem.* **2011**, *49*, 4065.
21. Nurulla, I.; Tanimoto, A.; Shiraishi, K.; Sasaki, S.; Yamamoto, T. *Polymer* **2002**, *43*, 1287.
22. Akpınar, H.; Balan, A.; Barana, D.; Ünver, E. K.; Toppare, L. *Polymer* **2010**, *51*, 6123.
23. Ozdemir, S.; Sendur, M.; Oktem, G.; Doğan, Ö.; Toppare, L. *J. Mater. Chem.* **2012**, *22*, 4687.
24. Nurioglu, A. G.; Akpınar, H.; Sendur, M.; Toppare, L. *J. Polym. Sci. Part A: Polym. Chem.* **2012**, *50*, 3499.
25. Wang, E.; Hou, L.; Wang, Z.; Hellström, S.; Mammo, W.; Zhang, F.; Inganäs, O.; Andersson, M. R. *Org. Lett.* **2010**, *12*, 4470.
26. Perzon, E.; Wang, X.; Admassie, S.; Ingana, O.; Anderson, M. R. *Polymer* **2006**, *47*, 4261.
27. Bin, Z. H.; Heng, N. J.; Jian, C.; Hua, Z. J.; Ning, Z.; Ming, P. S. *Chin. J. Chem. Res.* **2001**, *12*, 19.
28. Yuen, J. D.; Fan, J.; Seifert, J.; Lim, B.; Hufschmid, R.; Heeger, A. J.; Wudl, F. *J. Am. Chem. Soc.* **2011**, *133*, 20799.